Size Scale and Defect Engineered Nanostructures for Optimal Strength and Toughness

Final Report

PI: W.W. Gerberich, University of Minnesota

## I. Introduction

The goal of this research project was to develop realistic combinations of ceramics and/or semiconductors that simultaneously achieve high hardness (>40 GPa) and toughness (>400 MPa*$m^{1/2}$). While this is probably unrealistic for bulk material production due to inherent defects associated with processing, there is a very real opportunity for thin coatings in environments involving severe wear and/or dynamic penetration. This includes a wide range of industrial applications, including automotive, aircraft, electronics, manufacturing, and biomedical. To achieve this goal, the proposal outlined three primary objectives: (1) the development of physically based, dislocation models to understand the deformation of brittle materials, (2) the synthesis of model ceramic nanocomposites that demonstrate high hardness and toughness, and (3) the detailed understanding of the arrangements and types of dislocation structures in small volumes. This involved the uniaxial compression of Si nanovolumes (spheres and towers) using a combination of TEM *in situ* indentation and molecular dynamics simulations for objective (1), the deposition of Si-SiC core-shell nanotowers for objective (2), and the HR TEM analysis of deformed Si nanovolumes for objective (3). This report summarizes the substantial progress made on the first two of these objectives and the work that is currently underway to address objective (3).

## II. Uniaxial compression of Si nanospheres and towers

One of the major components of this research project was the deformation of silicon nanospheres and nanotowers through TEM *in situ* nanoindentation experiments. These consisted of a series of uniaxial compressions of hypersonic plasma particle deposition (HPPD) [1, 2] synthesized single crystal Si nanospheres ($d$=63-349 nm) on $Al_2O_3$ substrates and VLS grown Si(111) nanotowers ($d$=231-415 nm). Figure 1a,b gives an example of a 173 nm diameter Si nanosphere before and after compression. In the nanospheres, the oxide shell prevents the release of dislocations and leads to the formation of a back stress due to dislocation pile-up. The applied shear stress, $\tau$, needed to nucleate additional dislocations is thus increased and can be described by an Eshelby dislocation pile-up mechanism [3] as

$$\tau = \frac{\mu b N}{\pi (1-\nu) d} \tag{1}$$

# Report Documentation Page

*Form Approved*
*OMB No. 0704-0188*



| 1. REPORT DATE | 2. REPORT TYPE | 3. DATES COVERED |
|---|---|---|
| **07 MAR 2011** | **Final** | **30-04-2009 to 30-10-2010** |

4. TITLE AND SUBTITLE
**Size scale and defect engineered nanostructures for optimal strength and toughness**

5a. CONTRACT NUMBER
**FA23860914105**

5b. GRANT NUMBER

5c. PROGRAM ELEMENT NUMBER

6. AUTHOR(S)
**William Gerberich**

5d. PROJECT NUMBER

5e. TASK NUMBER

5f. WORK UNIT NUMBER

7. PERFORMING ORGANIZATION NAME(S) AND ADDRESS(ES)
**University of Minnesota,421 Washington Ave SE # 151,Minneapolis,MN,55455**

8. PERFORMING ORGANIZATION REPORT NUMBER
**N/A**

9. SPONSORING/MONITORING AGENCY NAME(S) AND ADDRESS(ES)
**AOARD, UNIT 45002, APO, AP, 96338-5002**

10. SPONSOR/MONITOR'S ACRONYM(S)
**AOARD**

11. SPONSOR/MONITOR'S REPORT NUMBER(S)
**AOARD-094105**

12. DISTRIBUTION/AVAILABILITY STATEMENT
**Approved for public release; distribution unlimited**

13. SUPPLEMENTARY NOTES

14. ABSTRACT
**The goal of this research project was to develop realistic combinations of ceramics and/or semiconductors that simultaneously achieve high hardness (>40 GPa) and toughness (>400 MPa*m1/2). While this is probably unrealistic for bulk material production due to inherent defects associated with processing, there is a very real opportunity for thin coatings in environments involving severe wear and/or dynamic penetration. This includes a wide range of industrial applications, including automotive, aircraft, electronics, manufacturing, and biomedical. To achieve this goal, the proposal outlined three primary objectives: (1) the development of physically based, dislocation models to understand the deformation of brittle materials, (2) the synthesis of model ceramic nanocomposites that demonstrate high hardness and toughness, and (3) the detailed understanding of the arrangements and types of dislocation structures in small volumes. This involved the uniaxial compression of Si nanovolumes (spheres and towers) using a combination of TEM in situ indentation and molecular dynamics simulations for objective (1), the deposition of Si-SiC core-shell nanotowers for objective (2), and the HR TEM analysis of deformed Si nanovolumes for objective (3). This report summarizes the substantial progress made on the first two of these objectives and the work that is currently underway to address objective (3).**

15. SUBJECT TERMS
**nanomaterials, Structural Materials**

| 16. SECURITY CLASSIFICATION OF: | | | 17. LIMITATION OF ABSTRACT | 18. NUMBER OF PAGES | 19a. NAME OF RESPONSIBLE PERSON |
|---|---|---|---|---|---|
| a. REPORT<br>**unclassified** | b. ABSTRACT<br>**unclassified** | c. THIS PAGE<br>**unclassified** | **Same as Report (SAR)** | **12** | |

**Standard Form 298 (Rev. 8-98)**
Prescribed by ANSI Std Z39-18

where $\mu$ is the shear modulus, $b$ is the Burgers vector, $N$ is the number of dislocations, $\nu$ is Poisson's ratio, and $d$ is the sphere diameter. Figure 1c shows the average flow stress as a function of diameter for nanospheres found using a geometric contact area. In addition, *ex situ* indentations of Si nanospheres are included from Mook et al. [4], where the flow stress was calculated based on an average between a geometric contact and cylindrical contact [4]. Assuming $\sigma_{flow} = 2\tau$ and using $\mu_{Si}$ = 60.5 GPa , $b_{Si}$ = 0.235 nm, and $\nu_{Si}$ = 0.218 [5], a least squares fit of Eqn. 1 gives ~60 dislocations (see Fig. 1). Future work with *in situ* TEM will more explicitly give the number of slip planes and their back stress.

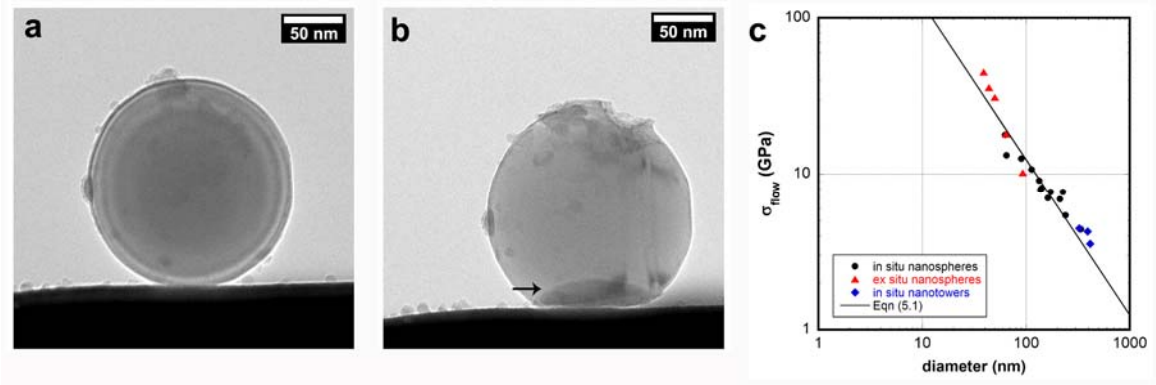


**Figure 1.** BF TEM of a 173 nm diameter Si nanosphere a) before and b) after TEM *in situ* compression, with the arrow in (b) highlighting evidence of residual plasticity. c) Flow stress as a function of nanosphere diameter.

Si nanospheres and nanotowers were also fractured *in situ* with a quantitative measurement of the fracture stress. Indents were run in displacement control, with 10 nm/s loading and unloading rates and a 5 sec hold at the peak load. Five spheres ($d$=113-349 nm) and three towers ($d$=231-415 nm) showed signs of fracture at failure. Figure 2a,b gives a representative example of the fracture of a 349 nm diameter Si nanosphere on an $Al_2O_3$ substrate. To determine the fracture toughness of the spheres and towers, a work per unit fracture area method was used since it accounts for dislocation plasticity and closely matches finite element modeling of the fracture toughness in Si nanotowers [6]. Fig. 2c summarizes the fracture toughness for the nanospheres and nanotowers along with *ex situ* nanosphere results from Mook et al. [4]. Here, the $d^{-1/2}$ can be explained

theoretically by balancing the crack extension force, $G_{IIc}$, with a dislocation resistive force, $F_R$, based on a dislocation line tension. With $\nu_{Si}$=0.218 and taking yield strength as the maximum value from Fig. 1c, the fracture toughness becomes

$$K_{Ic} = \frac{10}{9}\mu N b d^{-1/2} \quad . \qquad (2)$$

Eqn. 2 is shown in Fig. 2c as a solid line, with the same number of dislocations ($N$=60) as determined in Fig. 1. As with the strengthening argument proposed earlier, this result suggests that dislocations trapped in small volumes generate large back stresses and increase the yield strength. In addition, the piled up dislocations will act to shield the crack tip and inhibit crack growth, thus increasing the fracture toughness.

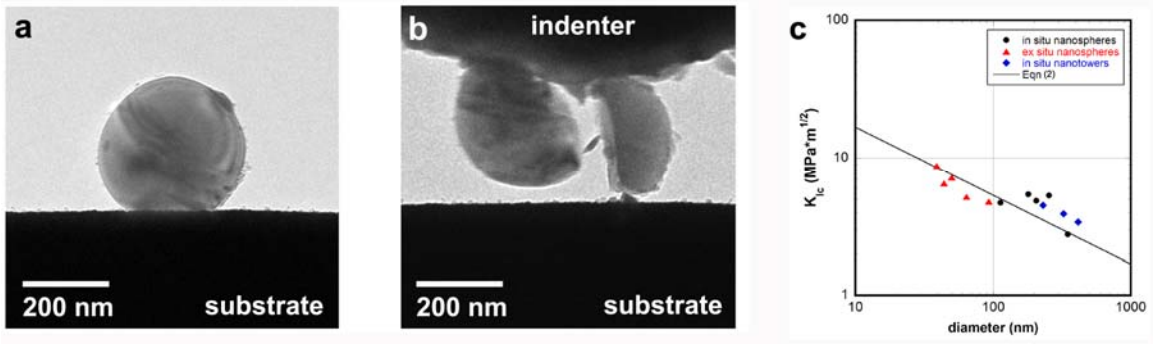


**Figure 2.** BF TEM of a 349 nm diameter Si nanosphere a) before and b) after TEM *in situ* compression, with (b) capturing a fracture event. c) Fracture toughness as a function of nanosphere diameter.

A third aspect of the deformation of Si in small volumes that was pursued was the role of phase transformation plasticity. The literature discussing the size effect on the Si phase transformation process [7-10] is much more limited (and inconclusive) than bulk studies. In the present data, the slope of the unloading curve for TEM *in situ* compression of Si nanospheres was found to decrease abruptly near the end of the unloading, creating an elbow (as shown in Fig. 3a). The location of the elbow can be defined as the point where the unloading curve deviates from the elastic-plastic power law fit. This type of feature is commonly seen during the indentation of silicon and has been attributed to the transformation of the high pressure β-Sn phase (Si II) of Si to an amorphous phase (a-Si) [11-13]. Knowing the contact area between the tip and the sphere, the pressure at which this event occurs in the 212 nm diameter nanosphere is 0.90 GPa. This is less than 1/6 of

the transition pressure for bulk Si(111) [12] and suggests an increased stability of Si II. At even smaller volumes, the elbow in the unloading slope disappears (see 65 nm diameter sphere in Fig. 3b). This represents a transition in the deformation mechanism to a dislocation plasticity dominated response below a critical length scale and is currently being investigated in more detail.

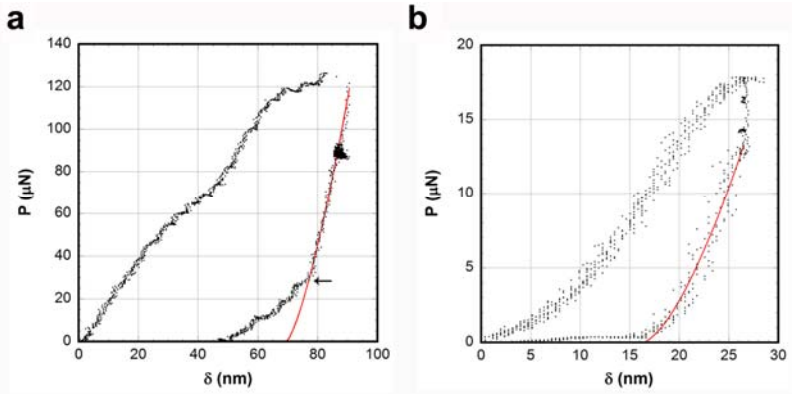


**Figure 3.** Load-displacement data for TEM *in situ* compression of Si nanospheres with diameters of a) 212 nm and b) 65 nm. The solid red line in each is an elastic-plastic unloading power law fit.

### III. Si-SiC core-shell nanocomposites

A second component of this research was in the development of nanocomposite materials based on the small scale strengthening and toughening mechanisms described earlier. The HPPD technique was used to deposit nanocrystalline (<20 nm grain size), 3C-SiC coatings with thicknesses of 100-200 nm on Si(111) nanotowers. The Si(111) towers were vapor-liquid-solid grown using chemical vapor deposition by collaborators at NIST [14]. Figure 4 gives representative images of the Si towers before and after deposition, with the towers attached to their original growth substrate in each case. Based on the DF TEM imaging, the composite structures shows the conformal nature of the coating, with good evidence that the appropriate adhesion has been achieved.

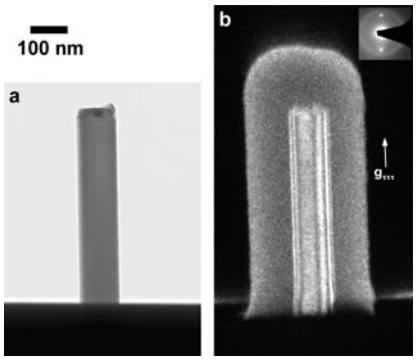


**Figure 4.** Examples of Si(111) nanotowers from batch B a) before (BF TEM) and b) after deposition of the SiC coating (DF TEM). The parallel lines running down the length of the Si in (b) are from thickness fringes.

The composite towers were then heat treated using rapid thermal annealing (RTA) for 20 sec at 900-1200°C in an Ar environment. Due to the mismatch in the coefficients of thermal expansion for the Si core and SiC shell, the Si core was left in residual compression following the RTA treatment. This compressive stress was measured using DF TEM strain contours, confocal Raman microscopy (CRM), and atomic force microscopy (AFM) as shown in Figures 5 and 6. Oscillations in DF TEM contrast (see Fig. 5a) originate from the base of the tower and show axial symmetry. This is consistent with an elastic strain profile for a capped annular coating, where the highest strain is at the top of the Si tower and relaxes at the base due to less confinement. CRM measurements used a 514.5 nm Ar laser focused perpendicularly onto the (111) surface of the Si nanotower. Measurements taken after RTA heat treatments showed a significant blue shift, with the strongest shift for the 1200°C treatment (see Fig. 5b). Assuming the Si towers are under a biaxial stress from the CTE mismatch with the SiC coating, this blue shift represents a compressive stress of 0.8-2.8 GPa (see Fig. 5c). While the magnitude of this stress is 3-5 times larger than an elastic estimate for concentric cylinders, the trend of increasing stress with increasing RTA temperature was verified by cross sectioning the towers along the radial axis and measuring the stress relaxation of the Si core. Figure 6a,b shows the composite surface that was cross sectioned with the focused ion beam. This produces a nominally flat surface, with the contrast in Fig. 6b due to the compositional difference between the core (Si) and shell (SiC). Following RTA treatment, the height of the extruded Si core was measured using AFM contact mode

imaging (Fig. 6c,d). With increasing RTA treatment temperature, there is an increased volume of Si extruded due to the higher CTE stresses on the core.

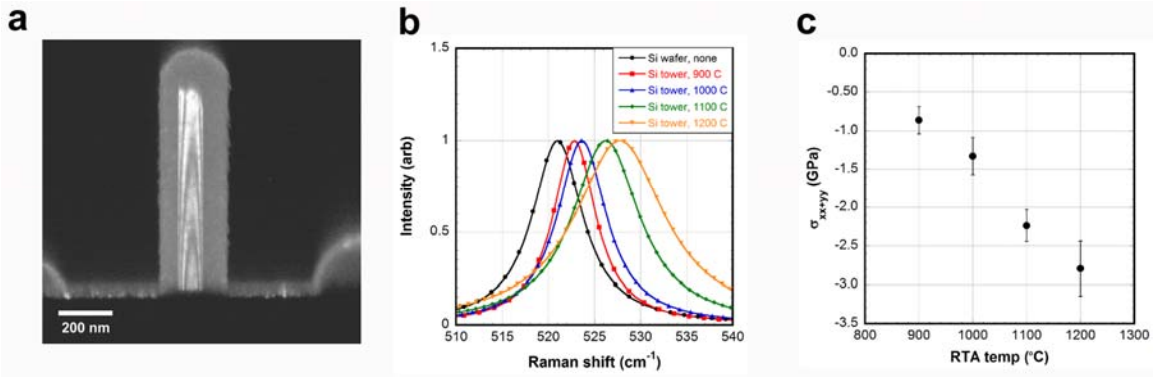


**Figure 5.** Evidence of residual stress in Si core, showing a) DF TEM strain contours, b) blue shift in the Raman Si response (normalized, Lorentzian fittings) for RTA treated (900-1200°C) composite towers, and c) the biaxial stress of the Si core as a function of RTA treatment temperature.

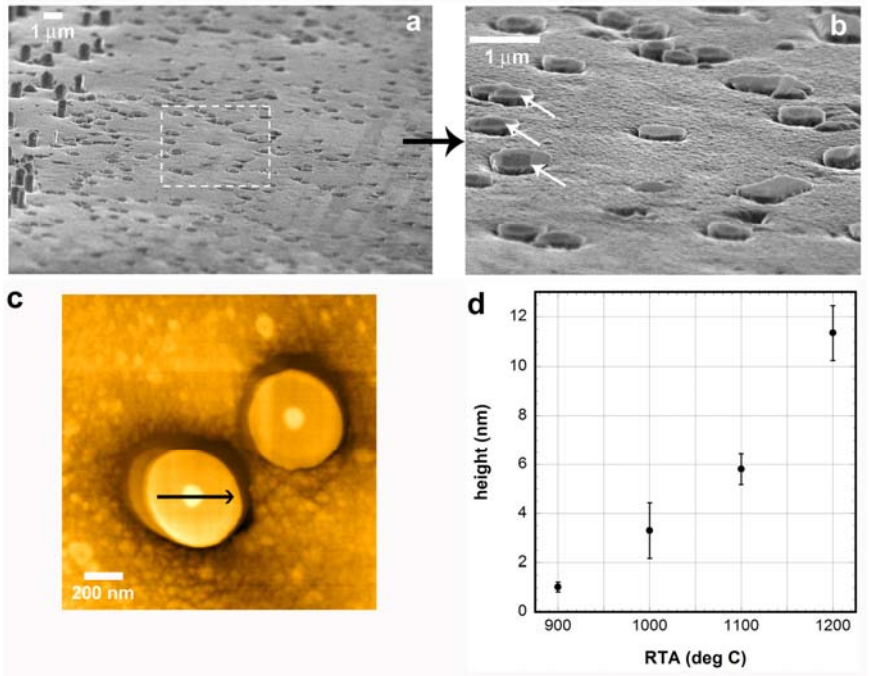


**Figure 6.** Additional evidence of residual stress on FIB cut composite Si towers, showing a,b) the FIB cut surface exposing the core-shell structure (two different magnifications), c) AFM contact mode imaging of a 1200°C RTA treated tower with an extruded Si core, and d) extruded core height as a function of RTA treatment temperature.

Considering the increased stability of Si II in small volumes (as shown in Section II) together with the high compressive stresses found in the Si–SiC core–shell composites (Section III), a new toughening mechanism for Si–SiC nanocomposites was proposed as follows. First, Si I nanospheres with diameters in the range of 100-1000 nm are dispersed in a SiC matrix and heat treated to 1100-1200°C. Based on Fig. 5c, this will leave the Si nanospheres under a compressive stress of close to 3 GPa. The composite is then loaded to a stress exceeding the critical stress needed for the Si I→II transition (~8-10 GPa). This can be done either under service conditions or by pre-stressing the composite. Upon unloading, the nanospheres will remain as Si II since the residual compressive stress is higher than the Si II→I transition pressure. When a crack forms in the composite, the tensile stress at the crack tip will destabilize the Si II and cause a transformation back to Si I. The volume expansion during this transformation will then act as a compressive stress to close the approaching crack, in same way transformations in partially stabilized zirconia (PSZ) have been shown to cause crack closure [15, 16]. If the tensile stress at the crack tip does not transform the Si II, the Si II nanospheres will act as either ductile inclusions for crack pinning or form voids due to the Si I→II contraction that will serve as crack arrest points. Thus, by controlling the length scale of the Si nanospheres, Si–SiC nanocomposites can be toughened by a combination of phase transformation and ductile phase reinforcement mechanisms.

## IV. MD simulations

Molecular dynamics simulations were used to investigate the mechanical properties resulting from the compression of silicon nanospheres, with a particular emphasis on determining the cause of the experimentally observed hardening behavior. The yielding properties observed within these modeled silicon nanospheres showed a high dependence on changes in the atomic potential, temperature, orientation and sphere size. These variations allowed for the study of numerous yielding behaviors, including phase transformations, dislocation nucleation and motion, and stacking fault formation and growth.

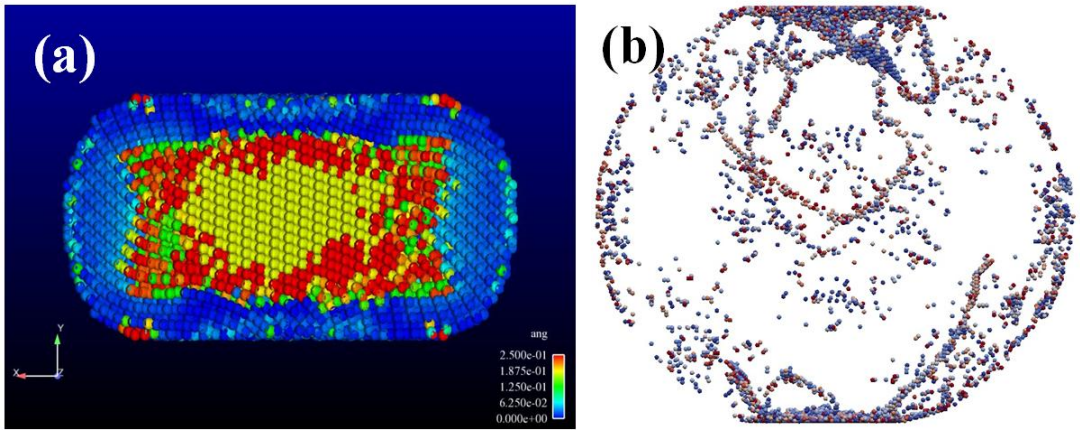


**Figure 7.** (a) Cross sectional image of a 10 nm sphere at 0 K using the Tersoff potential showing that the center has transformed into β-Sn (yellow). (b) Compression of a 34 nm diameter sphere at 300 K using the Stillinger-Weber potential reveals multiple dislocation loops that are seen to nucleate from the contact areas.

By relating the atomistic yielding mechanisms to the measured hardening behavior, it was found that the hardening behavior was independent of the pressure induced transformation to the β-Sn phase. Strong indications were also found that this hardening could be the result of dislocation interactions. To better investigate this, a million atom simulation was performed to maximize the number of dislocations. This revealed numerous dislocations that were able to interact resulting in a short period of hardening. The main limitation observed was that the dislocations quickly reach the sphere's surface and disappear due to the sphere's lack of an oxide layer. Currently, work is being done looking at how the presence of this oxide would affect the dislocation behavior.

## V. Conclusions

To date, the experiments performed have made substantial progress towards achieving the objectives of this project. Inverse length scale dependent relationships for strength and toughness in Si were identified based on dislocation pile-up and crack tip shielding mechanisms, respectively. In addition, a transition was identified in the deformation of Si under anisotropic loading below a critical size, showing increased stability of Si II and the transition at a critical length scale to dislocation dominated plasticity. By imposing a highly compressive stress on the Si core in Si-SiC composites,

the phase stability of Si II was applied to a new toughening mechanism in Si-SiC composites. Finally, MD simulations verified the presence of dislocation based plasticity during the deformation of small volumes of Si. Overall, these results demonstrate the importance of nanoscale confinement and localized stress in the design of mechanically robust nanocomposites.

Currently, experiments are underway to confirm the toughening mechanism proposed in Section III through a collaboration with EMPA Swiss Federal Laboratories. These experiments involve the SEM *in situ* compression of RTA treated Si-SiC composite towers to a pressure above the Si II transition. Upon release, we expect to see the Si II phase locked into place and will be able to verify this by the absence of an elbow in the load-displacement unloading curve and CRM analysis. In addition, we plan to FIB cut precracks in the composite towers and compress the towers *in situ* to observe the crack interaction with the compressively stressed Si core. Finally, we are beginning HR TEM experiments with *in situ* deformed Si nanotowers in the labs of Prof. Ikuhara to identify the types and arrangements of dislocations.

## VI. Program Metrics

This grant, in conjunction with NSF grant CTS-0506748, has resulted in 9 refereed publications (6 published, 1 in press, and 2 submitted), 2 published conference proceedings, 2 manuscripts in preparation, and 11 invited talks and seminars.

**Refereed publications:**


1. A.R. Beaber, S.L. Girshick, W.W. Gerberich, "Dislocation plasticity and phase transformations in Si-SiC core-shell nanotowers," Int. J. Fracture (submitted Aug 2010).

2. L.M. Hale, X. Zhou, J.A. Zimmerman, N.R. Moody, R. Ballarini, and W.W. Gerberich, "Phase transformations, dislocations and hardening behavior in uniaxially compressed silicon nanospheres," Acta Materialia (submitted Aug. 2010)

3. A.R. Beaber, J.D. Nowak, O. Ugurlu, W.M. Mook, S.L. Girshick, R. Ballarini, W.W. Gerberich, "Smaller is tougher," Philos. Mag. A (in press).

4. A. Beaber, W. Gerberich, "Alloys: Strength from modelling," Nat Mater 9 (2010) 698.

5. J.D. Nowak, A.R. Beaber, O. Ugurlu, S.L. Girshick, W.W. Gerberich, "Small size strength dependence on dislocation nucleation," Scripta Mater. 62 (2010) 819.

6. F. Östlund, K. Rzepiejewska-Malyska, K. Leifer, L.M. Hale, Y. Tang, R. Ballarini, W.W. Gerberich, J. Michler, "Brittle-to-Ductile Transition in Uniaxial Compression of Silicon Pillars at Room Temperature," Adv. Funct. Mater. 19 (2009) 2439.

7. L.M. Hale, X.W. Zhou, J.A. Zimmerman, N.R. Moody, R. Ballarini, W.W. Gerberich, "Molecular dynamics simulation of delamination of a stiff, body-centered-cubic crystalline film from a compliant Si substrate," J. Appl. Phys. 106 (2009) 083503.

8. N. Tymiak, D. Chrobak, W. Gerberich, O. Warren, R. Nowak, "Role of competition between slip and twinning in nanoscale deformation of sapphire," Phys. Rev. B 79 (2009) 174116.

9. M.J. Cordill, N.R. Moody, W.W. Gerberich, "The role of dislocation walls for nanoindentation to shallow depths," Int. J. Plast. 25 (2009) 281.

**Published proceedings:**

1. A.R. Beaber, Z.B. Gay, W.W. Gerberich, S.L. Girshick, "Residual stress toughening in ceramic nanocomposite coatings deposited by hypersonic plasma particle deposition," in: A. von Keudell, J. Winter, M. Böke, V. Schulz-von der Gathen (Eds.), ISPC 19, Bochum, Germany, 2009.

2. J.D. Nowak, A.R. Beaber, O. Ugurlu, W.W. Gerberich, O.L. Warren, "In-Situ Fracture of Silicon Nanoparticles," Microsc. Microanal. 15 (2009) 722.

**Publications in preparation:**

1. A.R. Beaber, O. Ugurlu, W.M. Mook, J. Michler, S.L. Girshick, W.W. Gerberich, "Stress mapping and fracture analysis in SiC coated Si nanowires," (in preparation, Sep 2010).

2. A.R. Beaber, S.L. Girshick, W.W. Gerberich, "A length scale dependent phase transformation in Si," (in preparation, Nov 2010).

**Invited talks and seminars:**

1. W.W. Gerberich, et al., “Plasticity: The impact of scale,” Int. Conf. on Metall. Coatings and Thin Films, 4/5/10.

2. W.W. Gerberich, et al., “High nanoscale strength and toughness in ceramics,” Departmental seminar, University of Kentucky, 5/13/10.

3. W.W. Gerberich, et al., “Fracture limitations: Dislocations and the size effect,” Materials Research Society Fall Meeting, Boston, MA, 12/2/09.

4. W.W. Gerberich, et al., “Nanoscale plasticity in brittle materials,” Materials Research Society Fall Meeting, Boston, MA, 12/1/09.

5. W.W. Gerberich, et al., “Strength limitations: Dislocations, transformation, and fracture,” Nanomechanical testing in materials research and development, Barga, Italy, 10/13/09.

6. W.W. Gerberich, et al., “Strength limitations: Dislocations, transformations, and the size effect,” U.C. Berkeley workshop, 8/11/09.

7. A.R. Beaber, et al., “Residual stress toughening in ceramic nanocomposite coatings deposited by hypersonic plasma particle deposition,” Int. Symp. on Plasma Chem., Bochum, Germany, 7/28/09.

8. W.W. Gerberich, et al., “Nanoscale effects on brittle fracture,” Int. Conf. Frac., Ottawa, Canada, 7/15/09.

9. A.R. Beaber, et al., “Residual stress induced toughening in SiC nanocomposite coatings,” Int. Conf. on Adv. Cer. and Comp., Daytona Beach, FL, 1/10/09.

10. W.W. Gerberich, et al., “Size scale effects on dislocation nucleation and fracture,” Symp. on Plasticity, St. Thomas, Virgin Islands, 1/6/09.

11. W.W. Gerberich, et al., “Nanoscale flow and fracture: Effect on the brittleness transition,” Materials Research Society Fall Meeting, Boston, MA, 12/1/08.

**VII. References**

1. N. Rao, B. Micheel, D. Hansen, C. Fandrey, M. Bench, S. Girshick, J. Heberlein, P. McMurry, "Synthesis of nanophase silicon, carbon, and silicon carbide powders using a plasma expansion process," J. Mater. Res. 10 (1995) 2073.

2. A.R. Beaber, L.J. Qi, J. Hafiz, P.H. McMurry, J.V.R. Heberlein, W.W. Gerberich, S.L. Girshick, "Nanostructured SiC by chemical vapor deposition and nanoparticle impaction," Surf. Coat. Technol. 202 (2007) 871.

3. J.D. Eshelby, F.C. Frank, H.H. Wills, F.R.N. Nabarro, "Equilibrium of linear arrays of dislocations," Philos. Mag. A 42 (1951) 351.

4. W.M. Mook, J.D. Nowak, C.R. Perrey, C.B. Carter, R. Mukherjee, S.L. Girshick, P.H. McMurry, W.W. Gerberich, "Compressive stress effects on nanoparticle modulus and fracture," Phys. Rev. B 75 (2007) 214112.

5. W.W. Gerberich, W.M. Mook, C.B. Carter, R. Ballarini, "A crack extension force correlation for hard materials," Int. J. Fracture 148 (2007) 109.

6. F. Östlund, K. Rzepiejewska-Malyska, K. Leifer, L.M. Hale, Y. Tang, R. Ballarini, W.W. Gerberich, J. Michler, "Brittle-to-Ductile Transition in Uniaxial Compression of Silicon Pillars at Room Temperature," Adv. Funct. Mater. 19 (2009) 2439.

7. D. Ge, A.M. Minor, E.A. Stach, J.W. Morris, "Size effects in the nanoindentation of silicon at ambient temperature," Philos. Mag. A 86 (2006) 4069.

8. A.M. Minor, E.T. Lilleodden, M. Jin, E.A. Stach, D.C. Chrzan, J.W. Morris, "Room temperature dislocation plasticity in silicon," Philos. Mag. A 85 (2005) 323.

9. S.H. Tolbert, A.B. Herhold, L.E. Brus, A.P. Alivisatos, "Pressure-induced structural transformations in Si nanocrystals: Surface and shape effects," Phys. Rev. Lett. 76 (1996) 4384.

10. P. Valentini, W.W. Gerberich, T. Dumitrica, "Phase transformation plasticity in silicon nanospheres," Phys. Rev. Lett. (2007).

11. V. Domnich, Y. Gogotsi, S. Dub, "Effect of phase transformations on the shape of the unloading curve in the nanoindentation of silicon," Appl. Phys. Lett. 76 (2000) 2214.

12. Y.B. Gerbig, S.J. Stranick, D.J. Morris, M.D. Vaudin, R.F. Cook, "Effect of crystallographic orientation on phase transformations during indentation of silicon," J. Mater. Res. 24 (2009) 1172.

13. J.E. Bradby, J.S. Williams, M.V. Swain, "In situ electrical characterization of phase transformations in Si during indentation," Phys. Rev. B 67 (2003) 9.

14. S. Krylyuk, A.V. Davydov, I. Levin, A. Motayed, M.D. Vaudin, "Rapid thermal oxidation of silicon nanowires," Appl. Phys. Lett. 94 (2009) 3.

15. D.J. Green, R.H.J. Hannink, M.V. Swain, Transformation toughening of ceramics, CRC Press, Boca Raton, 1989.

16. R.H.J. Hannink, P.M. Kelly, B.C. Muddle, "Transformation toughening in zirconia-containing ceramics," J. Am. Ceram. Soc. 83 (2000) 461.